Thermally tunable far-infrared metasurfaces enabled by $Ge_2Sb_2Te_5$ phase-change material

Riad Yahiaoui
Dept. of Physics & Astronomy
Howard University
Washington, DC USA
riad.yahiaoui@howard.edu

Joshua A. Burrow
Electro-Optics Department
University of Dayton
Dayton, OH USA
burrowj2@udayton.edu

Gary Sevison
Electro-Optics Department
University of Dayton
Dayton, OH USA
sevisong1@udayton.edu

Andrew Sarangan
Electro-Optics Department
University of Dayton
Dayton, OH USA
asarangan1@udayton.edu

Jay Mathews
Department of Physics
University of Dayton
Dayton, OH USA
jmathews1@udayton.edu

Imad Agha
Depts. Physics & Electro-Optics
University of Dayton
Dayton, OH USA
iagha1@udayton.edu

Augustine M. Urbas
Materials and Manufacturing Dir.
Air Force Research Lab
Dayton, OH USA
augustine.urbas@us.af.mil

Thomas A. Searles
Dept. of Physics & Astronomy
Howard University
Washington, DC USA
thomas.searles@howard.edu

***Abstract*— The development of active metadevices continues to present keystone challenges in fields of plasmonics and photonics. Here, we demonstrate an analogue of electromagnetically induced transparency (EIT) effect in a far-infrared metasurface device via near-field coupling of bright and quasi-dark resonances resonating at nearly the same frequency with contrasting line widths. The proposed metasurface was further optimized numerically in order to demonstrate a reconfiguration effect (frequency-shift of the spectral response). The tunability property of the device is achieved by incorporating a thin layer of $Ge_2Sb_2Te_5$ (GST), a temperature-driven phase change material (PCM). Theoretical analysis based on a coupled Lorentz oscillator model explains the physical mechanism in the proposed design and shows a good agreement with the observed results. Such active hybrid EIT metadevices could have applications in tunable slow-light effects, delay bandwidth management and ultrafast laser induced switching.**

Keywords*— *phase change materials, metasurfaces, slow light devices, electromagnetic induced transparency, far-IR

I. Introduction

Dynamically reconfigurable devices provide a controllable degree of freedom in the fields of light propagation, polarization control and information processing. In this context, intrinsic limitations posed by the operational bandwidths and losses of metamaterials (MMs) can be effectively mitigated through the incorporation of materials with tunable electrical and optical properties. The active control of the MM resonances has been achieved by integrating localized components, such as varactor diodes [1,2] or using electrically [3,4], optically [5,6] and thermally-driven materials [7,8]. Recent advances in atomic-layered two-dimensional (2D) materials, including graphene and transition metal dichalcogenides (TMDs) have attracted increasing attention and provided new perspectives in achieving novel active metadevices [9,10]. Compared to traditional semiconductors, 2D-layered materials have high carrier mobility, high surface conductivity and a very short carrier relaxation time [11,12]. Other promising candidates for active tunability are phase-change materials (PCMs), such as metal-oxide materials [13] and germanium-antimony-telluride $Ge_xSb_yTe_z$ (GST) alloys [14,15], which exhibit unique electrical and optical properties for various phase states excited using various stimuli methods. For example, the metal-oxide material vanadium dioxide (VO_2) is reported to exhibit a structural transition from an insulating monoclinic phase to a metallic rutile phase near room temperature at an ultrafast sub-picosecond timescale [16] and can be induced optically [17], electrically [18] or thermally [19]. These unique characteristics can dramatically improve the performance of MMs-based photonic devices.Ge2Sb2Te5 is the most commonly studied stoichiometry of the ternary alloy chalcogenide material. The rapid reversible phase transition between states presents abrupt changes in material properties. This reliable and promising phenomena shows great promise, not only for optical rewritable disks, but for tunable devices.

Tunable analogues of electromagnetically induced transparency (EIT) effect in metamaterials have also attracted a lot of interest due to their potential application in sensing [20,21], quantum information processing [22–24] and slow-light devices [25–28]. EIT is a nonlinear quantum interference phenomenon occurring in a three level atomic system leading to an extremely narrowband transparency window within a wide absorption line [24,29]. EIT-like effect in MMs usually occurs as a result of interference between a bright and a dark mode. The bright mode strongly couples with the incident light, while the dark mode couples weakly to the incident light. To realize EIT, it is required that both modes have similar resonant frequencies with a minor deviation in line width. In such a situation, the destructive interference of these modes induces a narrow transparency window between two distinct resonance dips [30].

In this paper, a tunable hybrid MM exhibiting an EIT-like effect is investigated in the far-infrared regime. In particular, a thin layer of thermally-controlled GST is utilized due to its ability to undergo a reversible switching between two different phases, a conductive crystalline phase (c-GST) and highly resistive amorphous phase (a-GST). The results show that the frequency range of transparency window can be continuously tuned upon varying the applied external temperature. The paper is organized as follows. We first present the design of the static far-IR MM without the phase change material and present the origin of the EIT-like response in the far-IR. Then, we show the tunability by varying the phase of the GST layer and compare it to the static case.

II. Static Far-Infared EIT-MM: Design and Results

The unit cell of the investigated metadevice is schematically shown in Fig. 1(a). It is composed of a metallic cut wire subresonator (CWR) in close proximity to a U-shaped subresonator (USR), each made of 100 nm-thick aluminum and deposited on the top side of a silicon (Si) substrate. The relevant geometrical dimensions of the unit cell are: $p_x = p_y =$ 6.4 µm, $l_1 =$ 4.1 µm, $l_2 =$ 3.2 µm, $l_3 =$ 2.3 µm and $w =$ 0.75 µm. Such periodic structure does not diffract normally incident electromagnetic radiation for frequencies less than 47 THz. Numerical calculations were carried out using the finite difference time domain (FDTD). In these calculations, the elementary cell of the designed metasurface was irradiated at normal incidence, under TE-*polarization* (E ∥ y-axis), as indicated in Fig. 1(a). Periodic boundary conditions were applied in the numerical model in order to mimic the functioning of a 2D infinite structure. In simulations, the silicon substrate was treated as a lossless dielectric with $\varepsilon =$ 11.9 and the aluminum (Al) was modeled as a lossy metal with a conductivity of 3.56×10^7 S/m.

Here, we investigate the EIT effect under the following conditions: (i) the resonance frequencies of the two coupled sub-resonators are nearly identical, with minor deviation (ii) they have significantly different resonance linewidths (strongly contrasting in Q-factors). The simulated transmission spectrum of the device is plotted in Fig. 1(b). One can observe a narrow transparency peak at around 14.9 THz with an amplitude as high as 65% between two resonance dips at around 14.32 THz and 15.5 THz, respectively, which is considered to be an EIT-like effect. Under the illumination of a linearly TE-polarized THz wave, each unit cell of the EIT-MM can be regarded as the combination of an outer U-shaped resonator (USR) supporting a symmetric Lorentz-type resonance at around 15.35 THz, which arises from the excitation of the radiative inductive-capacitive (LC) mode and an inner cut wire resonator (CWR) that exhibits a dipole type resonance at 15 THz (nearly the same frequency), as shown in Fig. 1(c). Despite the fact that both the resonators are directly excited by the incoming terahertz wave, the LC resonance with the lower Q-factor (Q = 4.96) serves as the "bright" mode and the dipole resonance displaying higher Q-factor (Q = 150) acts as the sub-radiant "quasi-dark" mode in the system. When the two resonators are arrayed within one unit cell, an EIT-like transparency window appears in the transmission spectrum instead of the transmission dips of the USRs and the CWRs.

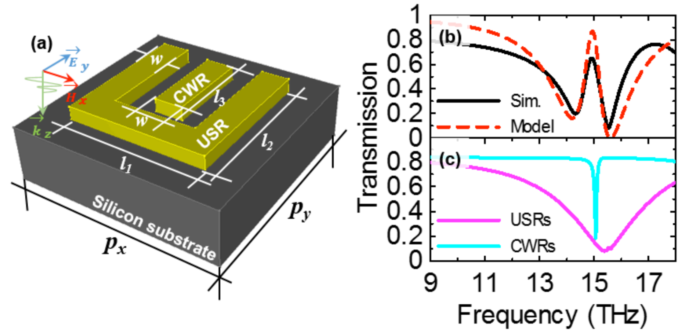

Fig. 1. (a) Unit cell of the designed metadevice with the corresponding electromagnetic excitation configuration. The relevant geometrical dimensions are: $p_x = p_y =$ 6.4µm, $l_1 =$ 4.1µm, $l_2 =$ 3.2µm, $l_3 =$ 2.3µm and $w =$ 0.75µm. (b) Measured dielectric constant ($\varepsilon = \varepsilon' + i\varepsilon''$) of the GST layer using ellipsometry and annealed at various temperatures between 130 °C and 220 °C. The phase transition (amorphous-to-crystalline) occurs at around 150°C. (c) Simulated transmission spectra of the sole USR array and the sole CWR array.

To demonstrate the validity of the underlying EIT effect, we used an analytical model based on the coupled oscillator theory described by the following set of equations [6,31]. Here, USR and CWR are designated as particles b and d, respectively, $(Q_b,\ q_b)$, $(M_b,\ m_d)$, $(\omega_b,\ \omega_d)$ $(\gamma_b,\ \gamma_d)$ and Ω are the effective charge, effective mass, resonance angular frequencies, loss factors and the coupling strength between (brigh, quasi-dark) particles.

Here, we consider both particles bright (x_b) and quasi-dark (x_d) interacting with the incident THz electric field $E = E_0 e^{i\omega t}$. In the above coupled equations, we substitute $q_d = Q_b/A$ and $m_d = M_b/B$, where A and B are dimensionless constants that dictate the relative coupling of incoming THz light with the particles. Now by expressing the displacements vectors for particles a and b as $x_a = c_a e^{i\omega t}$ and $x_b = c_b e^{i\omega t}$, we solve the above coupled equations (1) and (2) for x_a and x_b:

$$x_b = \frac{\frac{B}{A}\Omega^2 + (\omega^2 - {\omega_d}^2 + i\omega\,\gamma_d)}{\Omega^4 - (\omega^2 - {\omega_b}^2 + i\omega\,\gamma_b)(\omega^2 - {\omega_d}^2 + i\omega\,\gamma_d)}\,\frac{Q_b}{M_b}E \qquad (3)$$

and

$$x_d = \frac{\Omega^2 + \frac{B}{A}(\omega^2 - {\omega_b}^2 + i\omega\,\gamma_b)}{\Omega^4 - (\omega^2 - {\omega_b}^2 + i\omega\,\gamma_b)(\omega^2 - {\omega_d}^2 + i\omega\,\gamma_d)}\,\frac{Q_b}{M_b}E. \qquad (4)$$

The susceptibility (χ), which relates the polarization (P) of the particle to the strength of incoming electric field (E) is then expressed in terms of the displacement vectors as:

$$\chi = \frac{P}{\varepsilon_0 E} = \frac{Q_b x_b + q_d x_d}{\varepsilon_0 E} \qquad (5)$$

$$\chi = \frac{K}{A^2 B}\left(\frac{A(B+1)\Omega^2 + A^2\left((\omega^2\text{-}\omega_d{}^2)+B(\omega^2\text{-}\omega_b{}^2)\right)}{\Omega^4\text{-}(\omega^2\text{-}\omega_b{}^2+i\omega\,\gamma_b)(\omega^2\text{-}\omega_d{}^2+i\omega\,\gamma_d)} + i\omega\,\frac{A^2\,\gamma_d + B\,\gamma_b}{\Omega^4\text{-}(\omega^2\text{-}\omega_b{}^2+i\omega\,\gamma_b)(\omega^2\text{-}\omega_d{}^2+i\omega\,\gamma_d)}\right). \tag{6}$$

The simulated transmission in Fig. 1(b) is fitted by the imaginary part of the nonlinear susceptibility expression. In our fitting, the transmission coefficient is defined as T = 1-Im(χ) (given by the Kramer-Kronig relations), which is derived from the conservation of energy relation T+A = 1 (normalized to unity), where A = Im(χ) is the absorption (losses) within the medium. As the condition for EIT demands, in the analytical model, the resonance frequencies of the bright and the quasi-dark modes are kept constant ($\omega_b = \omega_d = 9.42\times10^{13}$ rad/ s), whereas their line widths differ by two orders of magnitude ($\gamma_d = 0.03\,\gamma_b$). A good agreement between the analytical data and the corresponding simulation is achieved for the coupling parameter $\Omega = 2.8 \times 10^{13}$ rad/s [see Fig. 1(b)].

III. Thermally Tunable EIT Metadevice

The unit cell of the tunable device is schematically shown in Fig. 2(a). A 100-nm-thick GST layer is inserted between the silicon substrate and the resonators while the other geometrical dimensions are kept constant. GST is a temperature-controlled PCM with an amorphous (a-GST) and discrete cubic crystalline (c-GST) phases with distinct electrical properties that can be reversibly switched between by applying either bias or incident optical pulses.

The dielectric constant (ε = ε′ + *i*ε″) of a RF sputtered 450 nm GST layer on glass was measured experimentally using a J. A. Wollam IR-VASE ellipsometer at various incident angles ranging from 50 - 75° and annealed at increasing temperatures between 130 °C and 220 °C then implemented in the numerical model. The phase transition (amorphous-to-crystalline) occurs around 150°C [see Fig. 2(b)]. Figure 2(c) shows the simulated transmission spectra of the device for different annealing temperatures of the GST layer. It is well-established that metamaterials are very sensitive to the surrounding dielectric environment. Hence, upon adding 100-nm-thick a-GST layer (in the amorphous phase without annealing) between the silicon substrate and the resonators, one can clearly observe that the transmission spectrum shifts to lower frequencies due to the increase in the capacitance of the structure [Fig. 2(c), red curve]. Similar behavior is observed in the crystalline phase of GST (c-GST), when further increasing the annealing temperature [Fig. 2(c), blue curve].

Of particular interest is the switching behavior and bandwidth modulation exhibited around the EIT window. With respect to the latter, the presence of the amorphous GST layer broadens and shifts the EIT window to lower frequency with respect to the static EIT-MM. Further, the window is considerably larger in bandwidth for the crystalline phase and shifted to above 16 THz. At 15 THz there is an ON/OFF

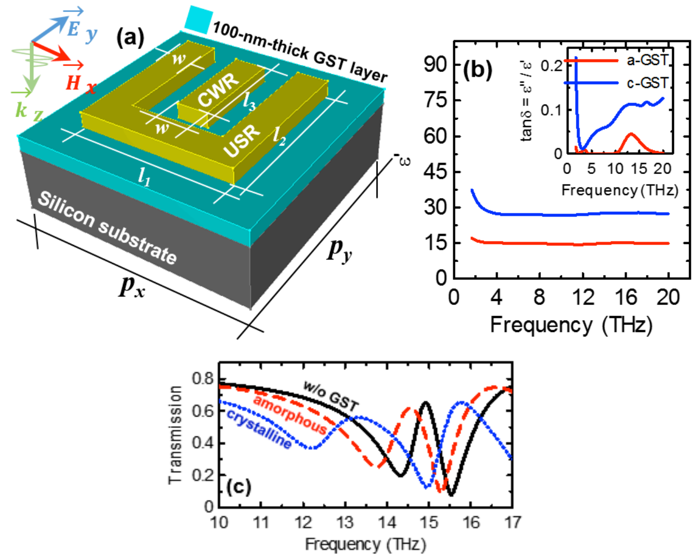

Fig. 2 (a) Unit cell of the designed GST-Si heterostructure metasurface active metadevice with the corresponding electromagnetic excitation configuration. The relevant geometrical dimensions remain unchanged: $p_x = p_y = 6.4$µm, $l_1 = 4.1$µm, $l_2 = 3.2$µm, $l_3 = 2.3$µm and $w = 0.75$µm. The thickness of aluminum is 100nm. (b) Measured dielectric constant (ε = ε′ + *i*ε″) of the GST layer using ellipsometry and annealed at various temperatures between 130 °C and 220 °C. The phase transition (a-GCT to c-GST) occurs at around 150°C. (c) Evolution of the simulated transmission spectra for different phases/annealing temperatures of the GST layer. The transmission spectrum without GST is also plotted for comparison (black curve).

capability exhibited between a transmission dip for the crystalline phase verses the original EIT window. We also would like to point out that this rich tunability and modulation can be further explored in higher frequencies up to optical frequencies by altering the substrate and unit cell geometry.

IV. Conclusion

In conclusion, we have demonstrated numerically and in the context of an analytical coupled oscillator model a frequency-agile EIT-like metadevice in the far-infrared regime. The frequency-tunability property is performed by incorporating a thin layer of GST temperature-driven phase change material (PCM). Our results pave the way towards the development of compact delay lines and slow-light active metadevices.

Acknowledgment

Funding for this research comes from the Air Force Office of Scientific Research (FA9550-16-1-0346) and the NSF (ECCS-1541959, ECCS-1710273, ECCS-1709200).

References

[1] I. V. Shadrivov, S. K. Morrison, and Y. S. Kivshar, “Tunable split ring resonators for nonlinear negative-index metamaterials,” Opt. Express, vol. 14, no. 20, pp. 9344–9349, Oct. 2006.

[2] Ourir, S. N. Burokur, R. Yahiaoui, and A. de Lustrac, “Directive metamaterial-based subwavelength resonant cavity antennas-applications for beam steering,” Comptes Rendus Phys., vol. 10, no. 5, pp. 414–422, Jun. 2009

[3] H. -T. Chen, W. J. Padilla, J. M. Zide, A. C. Gossard, A. J. Taylor, and R. D. Averitt "Active terahertz metamaterial devices," Nature, vol. 444, no. 7117, pp. 597–600, Nov. 2006.

[4] H.-T. Chen, S. Palit, T. Tyler, C. M. Bingham, J. M. O. Zide, J. F. O'Hara, D. R. Smith, A. C. Gossard, R. D. Averitt, W. J. Padilla, N. M. Jokerst, and A. J. Taylor, "Hybrid metamaterials enable fast electrical modulation of freely propagating terahertz waves," Appl. Phys. Lett., vol. 93, no. 9, pp. 091117-1–091117-3, Sep. 2008.

[5] H.-T. Chen, J. F. O'Hara, A. K. Azad, A. J. Taylor, R. D. Averitt, D. B. Shrekenhamer, and W. J. Padilla, "Experimental demonstration of frequency-agile terahertz metamaterials," Nat. Photon., vol. 2, pp. 295–298, Apr. 2008.

[6] R. Yahiaoui, M. Manjappa, Y. K. Srivastava, and R. Singh, "Active control and switching of broadband electromagnetically induce transparency in symmetric metadevices," Appl. Phys. Lett., vol. 111, no. 2, pp. 021101-1–021101-5, Jul. 2017.

[7] H. Němec, P. Kužel, F. Kadlec, C. Kadlec, R. Yahiaoui, and P. Mounaix, "Tunable terahertz metamaterials with negative permeability," Phys. Rev. B, vol. 79, no. 24, pp. 241108-1–241108-4, Jun. 2009.

[8] R. Yahiaoui, H. Němec, P. Kužel, F. Kadlec, C. Kadlec, and P. Mounaix, "Tunable THz metamaterials based on an array of paraelectric $SrTiO_3$ rods," Appl. Phys. A, vol. 103, no.3, pp. 689–692, Jun. 2011.

[9] W. Zheng, F. Fan, M. Chen, S. Chen, and S.-J. Chang, "Optically pumped terahertz wave modulation in MoS2-Si heterostructure metasurface," AIP Adv., vol, 6, no.7, pp. 075105-1–075105-8, Jul. 2016.

[10] Y. K. Srivastava, A. Chaturvedi, M. Manjappa, A. Kumar, G. Dayal, C. Kloc, and R. Singh, "MoS2 for ultrafast all-optical switching and modulation of THz Fano metaphotonic devices," Adv. Optical Mater., vol. 5, no. 23, pp. 1700762-1–1700762-8, Dec. 2017.

[11] R. Mas-Balleste, C. Gomez-Navarro, J. Gomez-Herrero, and F. Zamora, "2D materials: to graphene and beyond," Nanoscale, vol. 3, no.1, pp. 20–30, Jan. 2011.

[12] T. Korn, S. Heydrich, M. Hirmer, J. Schmutzler, and C. Schüller, "Low-temperature photocarrier dynamics in monolayer MoS2," Appl. Phys. Lett., vol. 99, no. 10, pp. 102109-1–102109-3, Sep. 2011.

[13] H.-S. P. Wong et al., "Metal–oxide RRAM," Proc. IEEE, vol. 100, no. 6, pp. 1951–1970, Jun. 2012.

[14] A. Saranagan, J. Duran, V. Vasilyev, N. Limberopoulos, I. Vitebskiy, and I. Anisimov, "Refractive optical limitier using GST phase change material with broad spectral band," IEEE Photoincs Journal, Accepted.

[15] M. J. Shu, et al., "Ultrafast terahertz-induced response of GeSbTe phase-change materials," Appl. Phys. Lett., vol. 104, no.25, pp. 251907-1–251907-4, Jun. 2014.

[16] A. Cavalleri, T. Dekorsy, H. H. W. Chong, J. C. Kieffer, and R. W. Schoenlein, "Evidence for a structurally driven insulator-to-metal transition in VO_2: A view from the ultrafest timescale," Phys. Rev. B, vol. 70, no. 16, pp. 161102-1–161102-4, Oct. 2004.

[17] A. Cavalleri, C. Tóth, C. W. Siders, J. A. Squier, F. Ráksi, P. Forget, and J. C. Kieffer, "Femtosecond structural dynamics in VO_2 during an ultrafast solid-solid phase transition," Phys. Rev. Lett., vol. 87, no. 23, pp. 237401-1–237401-4, Nov. 2001.

[18] G. Stefanovich, A. Pergament, and D. Stefanovich, "Electrical switching and Mott transition in VO_2," J. Phys. Condens. Matter, vol. 12, no. 41, pp. 8837–8845, Oct. 2000.

[19] D. C. Wang et al., "Switchable ultrathin quarter-wave plate in terahertz using active phase-change metasurface," Sci. Rep., vol. 5, pp. 15020-1–15020-9, Oct. 2015.

[20] N. Liu, T. Weiss, M. Mesch, L. Langguth, U. Eigenthaler, M. Hirscher, C. Sonnichsen, and H. Giessen, "Planar metamaterial analogue of electromagnetically induced transparency for plasmonic sensing," Nano Lett, vol. 10, no. 4, pp. 1103–1107, Sep. 2010.

[21] Z. G. Dong, H. Liu, J. X. Cao, T. Li, S. M. Wang, S. N. Zhu, and X. Zhang "Enhanced sensing performance by the plasmonic analog of electromagnetically induced transparency in active metamaterials," Appl. Phys. Lett., vol. 97, no. 11, pp. 114101-1–114101-3, Sep. 2010.

[22] J. E. Field, K. H. Hahn, and S. E. Harris, "Observation of electromagnetically induced transparency in collisionally broadened lead vapor," Phys. Rev. Lett., vol. 67, no. 22, pp. 3062–3065, Nov. 1991.

[23] K. J. Boller, A. Imamoğlu, and S. Harris, "Observation of electromagnetically induced transparency;" Phys. Rev. Lett., vol. 66, no. 20, pp. 2593–2596, May. 1991.

[24] M. Fleischhauer, A. Imamoğlu, J. P. Marangos, "Electromagnetically induced transparency: Optics in coherent media," Rev. Mod. Phys., vol. 77, no. 2, pp. 633–673, Jun. 2005.

[25] L. Zhu, F. Y. Meng, J. H. Fu, Q. Wu, and J. Hua "Multi-band slow light metamaterial," Opt. Express, vol. 20, no.4, pp. 4494–4502, Feb. 2012.

[26] V. Kravtsov, J. M. Atkin, and M. B. Raschke," Group delay and dispersion in adiabatic plasmonic nanofocusing," Opt. Lett., vol. 38, no. 8, pp. 1322–1324, Apr. 2013.

[27] F. Miyamaru, H. Morita , Y. Nishiyama, T. Nishida, T. Nakanishi, M. Kitano, and M. W. Takeda, "Ultrafast optical control of group delay of narrow-band terahertz waves," Sci. Rep., vol. 4, no., pp. 4346-1–4346-5, Mar. 2014.

[28] N. S. Ginsberg, S. R. Garner, and L. V. Hau, "Coherent control of optical information with matter wave dynamics," Nature, vol. 445, pp. 623-626, Feb. 2007.

[29] S. E. Harris, "Electromagnetically induced transparency," Phys. Today, vol. 50, no.7, pp. 36–42, Jul. 1997.

[30] K. M. Devi, A. K. Sarma, D. R. Chowdhury, G. Kumar, "Plasmon induced transparency effect through alternately coupled resonators in terahertz metamaterial," Opt Express., vol. 25, no. 9, pp. 10484–10493, May. 2017.

[31] F.-Y. Meng, Q. Wu, D. Erni, K. Wu, and J.-C. Lee, "Polarization-independent metamaterial analog of electromagnetically induced transparency for a refractive-index-based sensor," IEEE Trans. Microwave Theory Tech., vol. 60, no. 10, pp. 3013–3022, Oct. 2012.